

05.1;06.5;10

## Features of the behavior of laser ultrasonic signals near a hole in duralumin when exposed to two misaligned mechanical stresses

© A.L. Glazov, K.L. Muratkov

Ioffe Institute, St. Petersburg, Russia  
E-mail: glazov.holo@mail.ioffe.ru

Received September 3, 2021

Revised April 6, 2022

Accepted April 7, 2022

The effect of misaligned mechanical stresses on the excitation of ultrasonic vibrations by focused laser radiation near a small-diameter hole in aluminum alloy is investigated. The analysis of the behavior of the signal at various mutual angles and values of two uniaxial stresses is carried out. It is shown that at certain angles under the action of mechanical stresses, not only the contrast of laser ultrasound images changes, but also their rotation as a whole relative to the center of the hole can occur. The possibility of disappearance of the linear component of laser ultrasonic signals at certain characteristics of stress and appearance of a nonlinear component is also demonstrated.

**Keywords:** diagnostics, nondestructive evaluation, mechanical stress, laser ultrasound.

DOI: 10.21883/TPL.2022.06.53453.19013

The laser ultrasound (LU) techniques have recently demonstrated their efficiency in acquiring information on mechanical and thermoelastic properties of up-to-date materials, solid-state structures and thin films [1,2]. Intense investigation is being carried out of the LU technique application for diagnostics and nondestructive evaluation of products manufactured by innovative additive methods and 3D printing [3,4]. Also of great interest is studying the problems of behavior of LU signals from different-nature materials and influence of various-type defects on their characteristics. In solving such problems, the LU techniques possess such an advantage as nondestructive character and possibility of controlling not only surface characteristics of materials but also those of subsurface layers.

One of the most important characteristics defining serviceability of products is the level of mechanical stresses existing in them [5]. The necessity of controlling these stresses explains undertaking significant efforts aimed at investigation of the LU techniques promiseness in solving such problems. The LU techniques sensitivity to mechanical stresses was demonstrated for both ceramics [6,7] and metals [8,9]. In those works, the relationship between LU signals and stresses in materials was established using model samples.

Model experiments on analyzing the LU signals behavior near holes in stressed metals, which were performed in works [10,11], allowed us to determine not only qualitative but also quantitative characteristics of the LU signal-stress relationship for a number of metals. Notice that the above-mentioned studies were restricted to the case of mutually aligned external load and uniaxial residual stresses. In this geometry, the effect of uniaxial mechanical stresses is reduced to a mere variation in the LU image contrast in the region around the hole. The goal of this work was to study a more complex situation when the mentioned directions are

not aligned and formation of fundamentally new peculiar features of the LU images is possible.

As shown in [12], the uniaxial strain around the hole leads to formation of a stress field characterized by the below presented distribution of the first stress tensor invariant in the polar frame of reference  $(r, \varphi)$  with the origin in the center of the hole:

$$\sigma = \sigma_0(1 - 2a^2 \cos(2\varphi - 2\varphi_0)/r^2), \quad (1)$$

where  $\sigma_0$  is the stress far apart from the hole,  $a$  is the hole radius,  $\varphi_0$  is the angle between the uniaxial strain far from the hole and the  $\varphi = 0$  direction.

If external load  $P$  is applied at angle  $\alpha$ , an extra stress in the sample will be also defined by relation (1) provided  $\varphi_0$  is substituted by  $\alpha$  and  $\sigma_0$  is substituted by  $P$ . Then, according to the superposition principle, the total stress around the hole will be defined as

$$\sigma = P + \sigma_0 - 2a^2 \Sigma \cos(2\varphi - 2\beta)/r^2, \quad (2)$$

where

$$\Sigma = \sqrt{P^2 + \sigma_0^2 + 2P\sigma_0 \cos(2\alpha - 2\varphi_0)}, \quad (3)$$

$$\beta = 0.5 \arctan \frac{P \sin(2\alpha) + \sigma_0 \sin(2\varphi_0)}{P \cos(2\alpha) + \sigma_0 \cos(2\varphi_0)}. \quad (4)$$

In works [10,11], we have studied the case of the linear dependence of the LU signals on mechanical stresses. Based on the obtained results and equation (2), the LU signal may be presented as follows:

$$S = S_0(1 + b\sigma) = S_0(1 + b(P + \sigma_0) - 2ba^2 \Sigma \cos(2\varphi - 2\beta)/r^2), \quad (5)$$

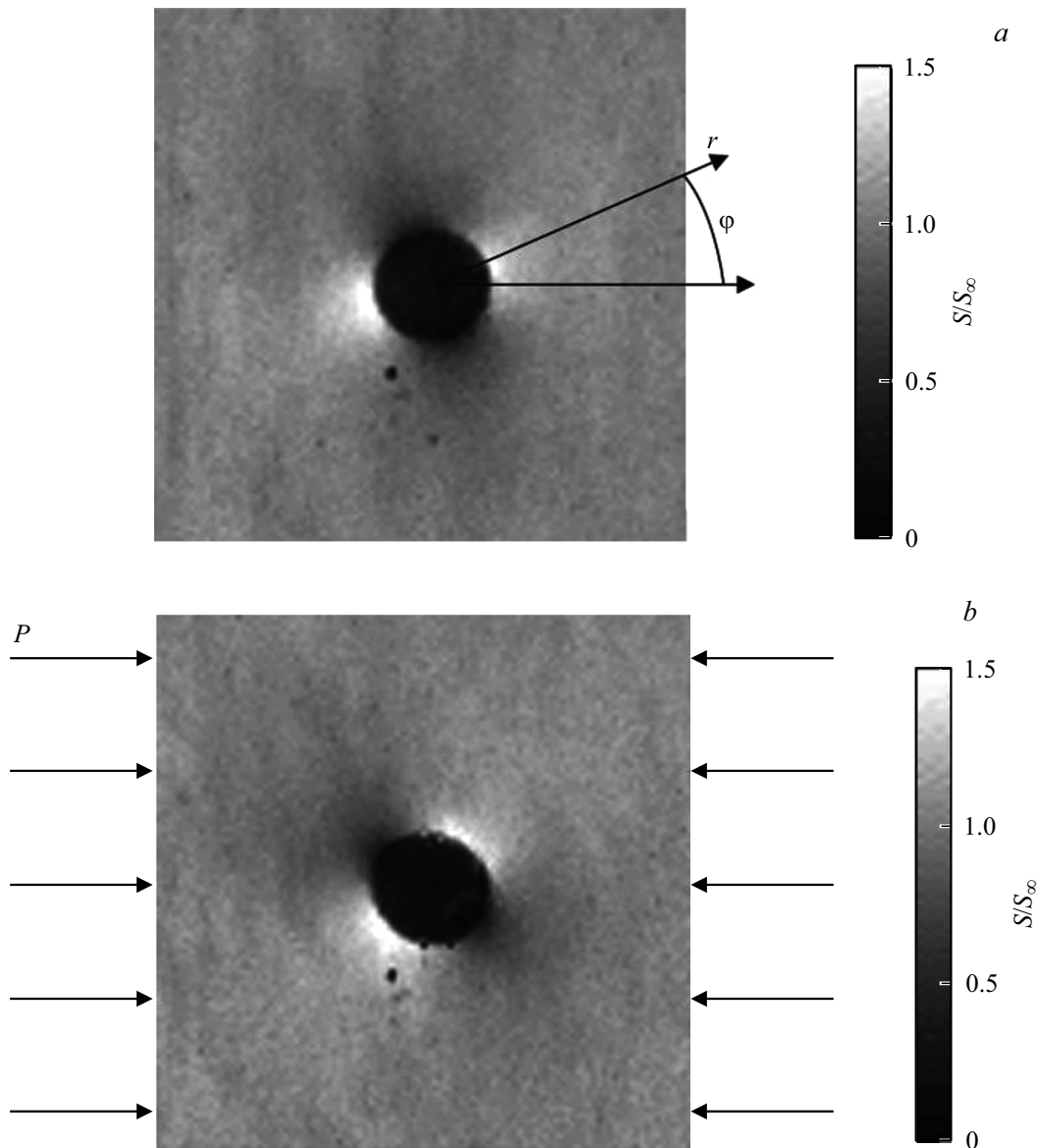


**Figure 1.** LU images of the duralumin sample surface. *a* — the sample in the initial state, *b* — the sample under uniaxial compressive load  $P = 20$  MPa (arrows indicate the direction of load application). The image size is  $1 \times 1$  mm.

where  $S_0$  is the signal from the stress-free sample,  $b$  is a certain proportionality factor depending on the material type,  $\sigma$  is the first stress tensor invariant.

Angle  $\varphi_0$  at  $P = 0$  and angle  $\beta$  under the load may be derived from experimental data on the LU images behavior near the hole. Then, using relation (4) and knowing load  $P$ , it is possible to determine the stress in the initial state:

$$\sigma_0 = P \sin(2\alpha - 2\beta) / \sin(2\beta - 2\varphi_0). \quad (6)$$

Factor  $b$  for the given material also may be determined from (5).

Analysis of relation (5) shows that, when the external and internal stresses are misaligned, fundamentally new features of the LU images behavior emerge. First, the presence of mechanical stresses in the sample can result

not only in variations in the LU images contrast, but also in their rotation about the hole center. Second, a nonlinear LU image may be obtained under the conditions of low contrast of linear LU images corresponding to the loads at which  $\Sigma$  is close to zero; that nonlinear LU image has a different structure, namely, each angular distribution contains not two maxima and two minima but four maxima and four minima. Below we demonstrate theoretical conclusions made based on experimental data on the LU signals behavior obtained on samples made from aluminum alloy D16 widely used in practice. This alloy was chosen because we have already shown for it the LU signal dependence on residual stresses [10,11]. The obtained conclusions are as a whole of a quite general character because of the earlier revealed relationship between LU

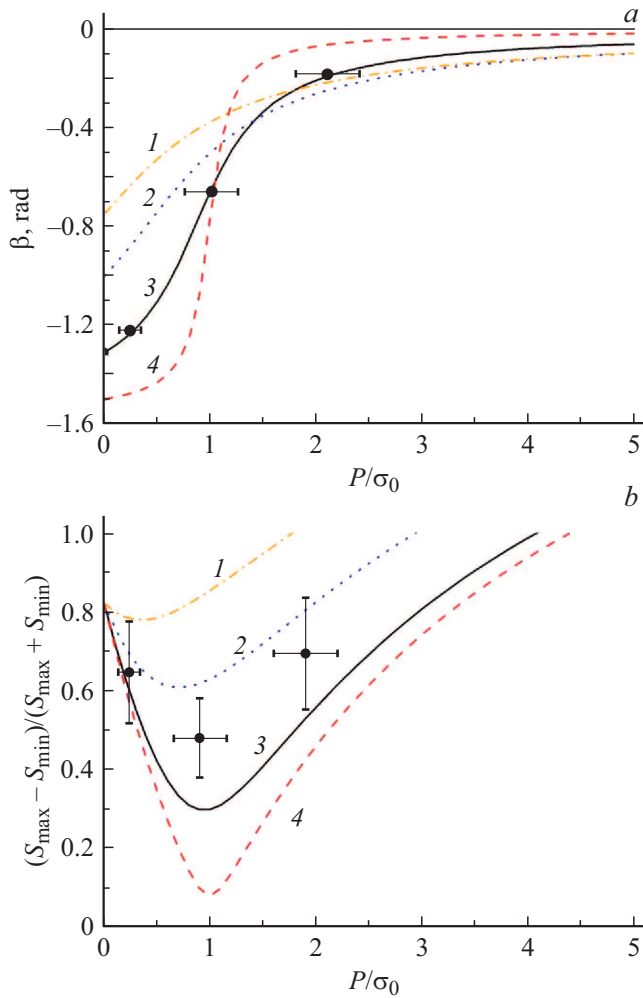


**Figure 2.** *a* — the symmetry axis angle of the signal  $\beta$  distribution calculated via (4) versus the  $P/\sigma_0$  ratio at different initial angles  $\varphi_0$ . *b* — the  $(S_{\max} - S_{\min})/(S_{\max} + S_{\min})$  signal variation contrast calculated via (5) at  $b\sigma_0 = 0.7$ . Curves in both panels correspond to angles  $\varphi_0 = -0.75$  (1),  $-1.0$  (2),  $-1.31$  (3) and  $-1.5$  (4). Points indicate relevant values found by approximating experimental LU images.

signals and internal stresses and of the solution of an elasticity theory problem not associated with a specific material.

The sample was a rectangular parallelepiped  $8.8 \times 7.1 \times 4.0$  mm in size. In the center of the major face there was drilled a blind hole with the effective diameter at the surface of  $0.11 \pm 0.01$  mm. The experiment consisted in irradiating the sample surface with a focused laser beam 532 nm in wavelength which was amplitude-modulated with the frequency of 101.4 kHz, and in detecting thermoelastically induced acoustic vibrations of the sample. The experimental setup layout is given in [13]. The mean power of radiation falling on the sample surface was 40 mW, while the spot diameter on the surface was  $15 \mu\text{m}$ . The mean temperature in the spot center was estimated as  $55^\circ\text{C}$ . Acoustic vibration was measured at the sample back side

by using a piezoelectric sensor having a close resonance frequency; the sensor was pressed against the surface via acoustic gel. An electrical signal proportional to the drift velocity of the sample back side was detected in scanning the surface around the hole in two perpendicular directions. During scanning, the uniaxial compressive load was applied to the samples. The sample LU images obtained in this way in both the initial state and under the load of  $20 \pm 2$  MPa are presented in Fig. 1. The images are normalized to mean signal  $S_\infty$  measured far from the hole. Fig. 1, *a* shows that the sample in the initial state exhibits a peculiar double-uniaxial signal distribution with the axes inclined at angles  $-1.31 \pm 0.01$  rad and  $\pi/2 - 1.31 \pm 0.01$  rad. If a load of 20 MPa is applied (Fig. 1, *b*), the symmetry axes rotate by the angle of  $+0.57$  rad. Thus, following the above designations, obtain  $\varphi_0 = -1.31 \pm 0.01$  rad,  $\beta = -0.77 \pm 0.01$  rad. The given errors are standard deviations of the signal distribution approximation via relation (5). Using (6), obtain  $\sigma_0 = -20 \pm 3$  MPa under the assumption that  $\alpha = 0$ . We have also obtained LU signals at other external loads. Fitting with respect to four sets of signals simultaneously at  $P = 0, 5, 20$  and  $41$  MPa provides the same stress values (within the accuracy range). Notice that in the general case the obtained quantity is a difference between two main components of the stress tensor, i.e., this may be either the compressive stress along the axis at angle  $\varphi = -1.31$  rad, or tensile stress of the same magnitude along the perpendicular axis, or their difference. Fig. 2, *a* presents the  $P/\sigma_0$  ratio dependence of the signal distribution symmetry axis angle  $\beta$  calculated via (4) at different angles  $\varphi_0$ , including that of  $-1.31$  rad. The points represent experimental data with indicating the obtained  $\sigma_0$ . One can see that the maximal sensitivity in determining the initial stress via the image rotation angle takes place at  $P \approx \sigma_0$ . At high loads, orientation of the LU image symmetry axis will be close to that of the external load ( $\beta \approx \alpha$ ).

Now consider the behavior of the LU signal amplitude in the vicinity of the hole in dependence on the external load. Fig. 2, *b* shows the contrast of the  $(S_{\max} - S_{\min})/(S_{\max} + S_{\min})$  signal variation versus the  $P/\sigma_0$  ratio, which was calculated at the same angles, i.e., at  $\varphi_0$  and  $b\sigma_0 = 0.7$ . Here  $S_{\max}$  and  $S_{\min}$  are the maximal and minimal amplitudes of the signal near the hole edge. In this figure, the points represent the amplitudes of signals obtained by approximating the images using relation (5). The curves have minima at  $P \approx \sigma_0$ , i.e., the signal distribution is expected to become more uniform. However, when the above-specified load is applied, the LU image exhibits a signal angular distribution corresponding to  $\cos(4\varphi)$ . Fig. 3, *a* presents an example of such an image at  $P = 28$  MPa. This means that, when the linear term disappears, the square-law stress dependence emerges [11], which results in the signal increase at both the compressive and tensile stresses. What is important is that, as shown in Fig. 2, *b*, the linear component again increases with further increasing load, and the image takes the form presented in

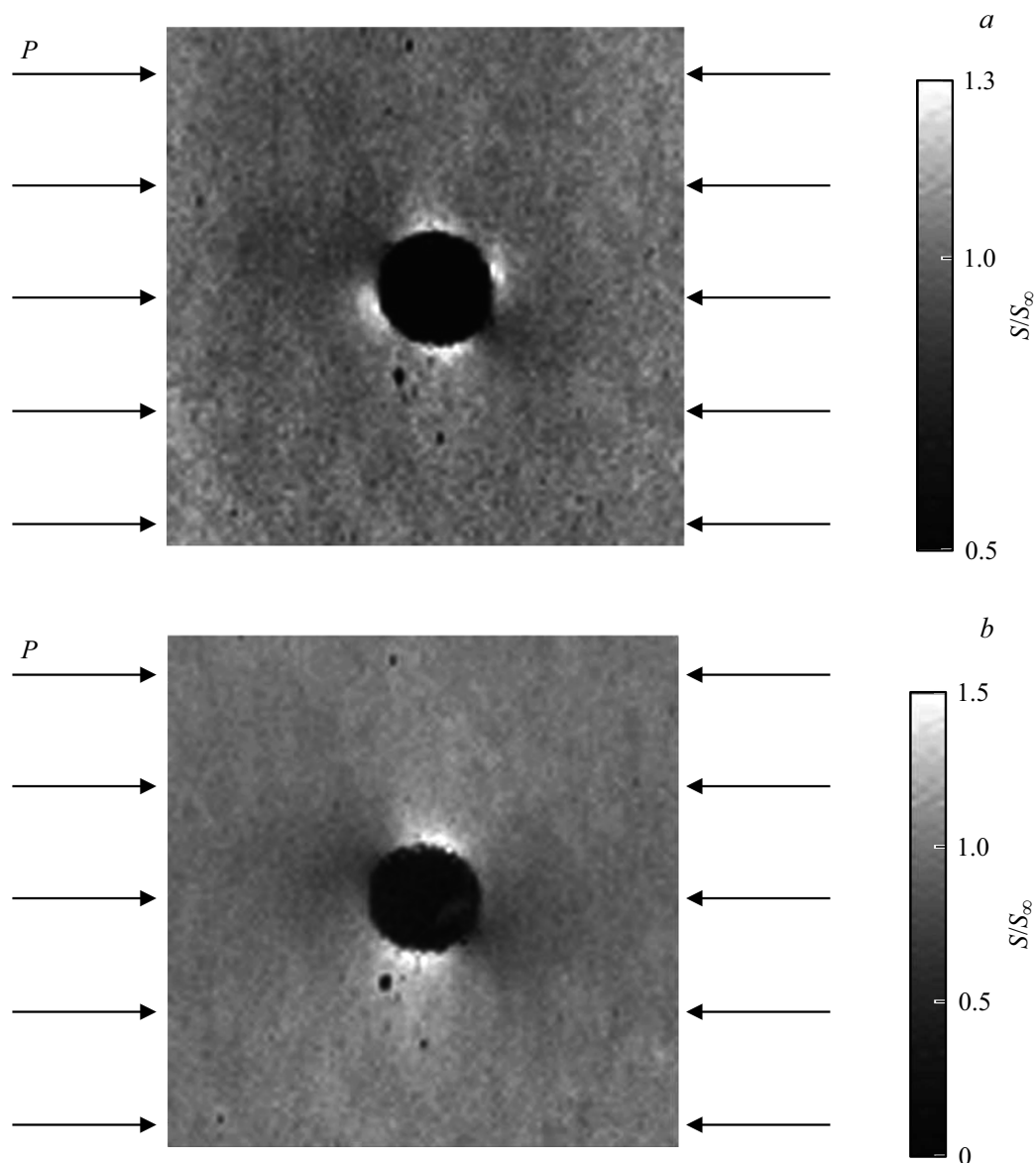


**Figure 3.** LU images of the duralumin sample surface. *a* — the sample under the uniaxial compressive load of 28 MPa, *b* — the sample under the uniaxial compressive load of 41 MPa. The image size is  $1 \times 1$  mm.

Fig. 3, *b* for the load of 41 MPa. Orientation of one of the symmetry axes becomes already close to that of the external load, and no image rotation takes place. In the general case, the presence of the nonlinear component in an LU image may be revealed by extra digital processing, for instance, by comparing the approximations of the 2D LU signal distribution by the linear and square-law functions [11].

In conclusion let us emphasize that the presented behavior of the LU signal amplitudes allows estimation of the residual stresses by measuring angles of only the main deformation tensor axes corresponding to the positions of maxima and minima of the detected signals. This paper has also experimentally demonstrated for the first time the nonlinear dependence of the excited LU vibration on mechanical stresses.

### Financial support

The study was accomplished in the framework of State Assignment of the RF Ministry of Science and Higher Education (Project № 0040-2019-0019).

### Conflict of interests

The authors declare that they have no conflict of interests.

### References

- [1] A. Setiawan, G.B. Suparta, M. Mitrayama, W. Nugroho, *Int. J. Adv. Sci. Eng. Inform. Technol.*, **7** (6), 2189 (2017). DOI: 10.18517/ijaseit.7.6.2816

- [2] D.D. Markushev, J. Ordonez-Miranda, M.D. Rabasović, M. Chirtoc, D.M. Todorović, S.E. Bialkowski, D. Korte, M. Franko, *Eur. Phys. J. Plus.*, **132** (1), 33 (2017). DOI: 10.1140/epjp/i2017-11307-2
- [3] C. Millon, A. Vanhoye, A.F. Obaton, J.D. Penot, *Weld. World*, **62** (3), 653 (2018). DOI: 10.1007/s40194-018-0567-9
- [4] Y. Zhan, H. Xu, W. Du, C. Liu, *Ultrasonics*, **115**, 106466 (2021). DOI: 10.1016/j.ultras.2021.106466
- [5] I.A. Birger, *Ostatochnye napryazheniya* (LENAND, M., 2015).(in Russian)
- [6] K.L. Muratkov, A.L. Glazov, D.N. Rose, J.E. Dumar, *J. Appl. Phys.*, **88** (5), 2948 (2000). DOI: 10.1063/1.1287526
- [7] A.L. Glazov, K.L. Muratkov, *Tech. Phys. Lett.*, **47**, 605 (2021). DOI: 10.1134/S1063785021060225.
- [8] A.Yu. Devichenskii, A.M. Lomonosov, S.E. Zharinov, V.G. Mikhalevich, M.L. Lyamshev, T.O. Ivanova, N.S. Merkulova, *Acoust. Phys.*, **55** (1), 61 (2009). DOI: 10.1134/S1063771009010060
- [9] N.B. Podymova, I.E. Kalashnikov, L.K. Bolotova, L.I. Kobel'eva, *Ultrasonics*, **108**, 106235 (2020). DOI: 10.1016/j.ultras.2020.106235
- [10] A.L. Glazov, K.L. Muratkov, *Tech. Phys. Lett.*, **45** (9), 902 (2019). DOI: 10.1134/S1063785019090049.
- [11] A.L. Glazov, N.F. Morozov, K.L. Muratkov, *Tech. Phys. Lett.*, **46** (2), 171 (2020). DOI: 10.1134/S1063785020020200.
- [12] S. Timoshenko, J.N. Goodier, *Theory of elasticity* (McGraw–Hill, N.Y., 1951), p. 78.
- [13] A.L. Glazov, K.L. Muratkov, *J. Phys.: Conf. Ser.*, **1697**, 012186 (2020). DOI: 10.1088/1742-6596/1697/1/012186